metals

Article

Effect of Ceramic Content on the Compression Properties of TiB₂-Ti₂AlC/TiAl Composites

Shili Shu [1,2], Cunzhu Tong [2], Feng Qiu [1,3],* and Qichuan Jiang [1],*

[1] Key Laboratory of Automobile Materials (Ministry of Education), Department of Materials Science and Engineering, Jilin University, Changchun 130025, China; E-Mail: shushili@ciomp.ac.cn

[2] State Key Laboratory of Luminescence and Applications, Changchun Institute of Optics, Fine Mechanics and Physics, Chinese Academy of Sciences, Changchun 130012, China; E-Mail: tongcunzhu@ciomp.ac.cn

[3] Department of Mechanical Engineering, Oakland University, Rochester, MI 48309, USA

* Authors to whom correspondence should be addressed; E-Mails: qiufeng@jlu.edu.cn (F.Q.); jqc@jlu.edu.cn (Q.J.); Tel./Fax: +86-431-8509-5592 (F.Q.); +86-431-8509-4699 (Q.J.).

Academic Editor: Ana Sofia Ramos

Abstract: *In situ* synthesized TiB₂-reinforced TiAl composites usually possess high strength. However, it is very expensive to use B powder to synthesize TiB₂ particles. Moreover, the strength enhancement of TiB₂/TiAl composite is generally at the cost of plasticity. In this study, *in situ* dual reinforcement TiB₂-Ti₂AlC/TiAl composites were fabricated by using B₄C powder as the B and C source, which greatly reduces the potential production cost. The 6 vol. % TiB₂-Ti₂AlC/TiAl composite fabricated by using the Ti-Al-B₄C system shows greatly improved compressive properties, *i.e.*, 316 MPa and 234 MPa higher than those of TiAl alloy and with no sacrifice in plasticity.

Keywords: TiAl; intermetallics; composite; compression properties

1. Introduction

Composite technology, *i.e.*, introducing stiff and hard particle reinforcements, is an effective approach to improve the strength of TiAl alloy [1–5]. TiB₂ and Ti₂AlC are the two most frequently-used reinforcing particles in TiAl matrix composites [4–6]. It has been reported that TiB₂ particles can

effectively enhance the strength of TiAl alloy [7–10]. However, the strength enhancement of the TiAl matrix composite caused by the addition of TiB_2 particles is usually at the cost of plasticity [7–10]. In contrast to TiB_2, Ti_2AlC ceramic combines unusual properties of both metals and ceramics, that is it possesses both plasticity and strength [11–13]. Although the enhancement effect of Ti_2AlC is relatively weaker than that of TiB_2, Ti_2AlC particles could improve the strength of the TiAl alloy and, at same time, with no great plasticity damage [14]. Therefore, introducing TiB_2 and Ti_2AlC particles simultaneously into TiAl matrix is expected to fabricate the *in situ* dual reinforcement TiB_2-Ti_2AlC/TiAl composite with further improved strength and also excellent plasticity.

The most direct idea to fabricate *in situ* dual reinforcement TiB_2-Ti_2AlC/TiAl composite is using the Ti-Al-B-C system. However, B powder is very expensive, which limits its potential application in industrial practice. Thus, it is necessary to find another material to use as the B source instead of B powder. As is known, the cost of B_4C powder is at least 20-times less expensive than that of B powder. Meanwhile, B_4C powder can offer C to synthesize Ti_2AlC particles. Thus, it is a more cost-effective way to fabricate the *in situ* dual reinforcement TiB_2-Ti_2AlC/TiAl composite by using B_4C as the B and C source.

Recently, several methods have been applied to fabricate TiAl matrix composites. Van Meter *et al.* [7] fabricated 40 vol. % and 50 vol. % TiB_2/TiAl composites by the method of powder metallurgy (P/M). The compression strength of the composites was reported in the range of 2484–2866 MPa, and fracture strain was in the range of 0.4%−1.7%. Bohn *et al*. [9] fabricated Ti_5Si_3/TiAl composites by the method of hot isostatic pressing (HIP). Compression strength reached up to 2680 MPa for the sample with a mean grain size of 170 nm, while fracture strain was about 1.2%. Yang *et al.* [15] fabricated Ti_2AlC/TiAl composites by the method of spark plasma sintering (SPS). The compression strength of the composites reached 2058 MPa, and the fracture strain was about 0.16%. Compared with these above methods, the method of combustion synthesis and hot press consolidation represents an *in situ* processing technique for the preparation of composites, which takes advantage of the low energy requirement, cleaner particle-matrix interface, one-step forming process, density and high purity of the products. Consequently, the fabricated composites would possess better comprehensive properties.

In our previous work [16], we focused on the issues of the effect of B_4C size on the fabrication of *in situ* TiB_2-Ti_2AlC/TiAl composites. It was concluded that just when the size of B_4C particles is reduced to 3.5 μm, pure *in situ* TiB_2-Ti_2AlC/TiAl composites could be successfully fabricated. However, the effect of the content of synthesized ceramic particles on the compression properties of TiB_2-Ti_2AlC/TiAl composites was not discussed. Thus, in this work, under the basis of the mentioned research work, the B_4C particles with a size of 3.5 μm were directly used to fabricate TiB_2-Ti_2AlC/TiAl composites with different contents of the synthesized ceramic particles. The effect of the content of synthesized ceramic particles on the compression properties and work-hardening capacity of TiB_2-Ti_2AlC/TiAl composite was investigated. Moreover, the reinforcing effect of the TiB_2-Ti_2AlC particulates synthesized from Ti-Al-B_4C and Ti-Al-B-C systems was compared.

2. Experimental Section

Starting materials were made from commercial powders of Ti (99.5% purity, ~25 μm), Al (99% purity, ~74 μm), B_4C (99.5% purity, ~3.5 μm), B (98% purity, ~3 μm) and carbon black (99.9% purity). The powders of Ti, Al and B_4C (Ti-Al-B_4C system) corresponding to nominal 2, 4, 6 and 8 vol. % TiB_2-Ti_2AlC/TiAl composites were mixed sufficiently by ball milling for 8 h at a low speed (~35 rpm) in a conventional planetary ball-miller. Both the pot and balls were made of stainless steel, and the mass ratio of ball to powders was 20:1–25:1. Then, the mixed powders were cold pressed into cylindrical compacts using a stainless steel die. In addition, the powders of Ti, Al, B and carbon black (Ti-Al-B-C system) corresponding to nominal 6 vol. % TiB_2-Ti_2AlC/TiAl composite were also mixed and pressed into cylindrical compact, which was used to compare to the composites fabricated by using the Ti-Al-B-C system. Unless specified otherwise, the composites were fabricated from the Ti-Al-B_4C system. The powder compact of 28 mm in diameter and approximately 36 mm in height was contained in a graphite mold, which was put into a self-made vacuum thermal explosion furnace. The heating rate of the furnace was about 30 K/min, and the temperature in the vicinity of the center of the compact was measured by Ni-Cr/Ni-Si thermocouples. When the temperature measured by the thermocouples suddenly rose rapidly, indicating that the sample should be ignited, the sample was quickly pressed just when it was still hot and soft. Pressure (~50 MPa) was maintained for 10 s, and then, the product was cooled down to ambient temperature at a cooling rate of ~10 K/min.

The phase constituents of composites were examined by X-ray diffraction (XRD, Rigaku D/Max 2500PC, Rigaku Corporation, Tokyo, Japan) with Cu Kα radiation. Microstructures were studied using scanning electron microscopy (SEM, Evo18, Carl Zeiss, Oberkochen, Germany) equipped with an energy-dispersive spectrometer (EDS, Oxford Instruments, Oxford, UK).The density of each sample was measured three times by Archimedes' water-immersion method, and average values are listed in Table 1.The cylindrical specimens with a diameter of 3 mm and a height of 6 mm were used for compression tests, and the loading surface was polished parallel to the other surface. Uniaxial compression tests were carried out under a servo-hydraulic materials' testing system (MTS, MTS 810, MTS Systems Corporation, Minneapolis, MN, USA) with a strain rate of 1×10^{-4} s^{-1}.

3. Results and Discussion

3.1. Phase Constituents and Microstructures

In order to identify the synthesized ceramic particles, the phase constituents of the composites were examined by XRD. Figure 1 shows the X-ray diffraction results of the composites fabricated from the Ti-Al-B_4C system. Actually, due to the limitation of the detection capacity of XRD, no ceramic phases, but the γ-TiAl and $α_2$-Ti_3Al phases, were detected in the samples with 2, 4 and 6 vol. % nominal ceramic contents. In the sample with a high content of ceramic particles (the nominal ceramic content is 8 vol. %), the TiB_2 and Ti_2AlC phases were detected besides the γ-TiAl and $α_2$-Ti_3Al phases. The combustion synthesis reaction in the Ti-Al-B_4C system is complete, and no trace of residual B_4C particles was found, which indicated that TiB_2 and Ti_2AlC particles could be synthesized simultaneously in the Ti-Al-B_4C system and that *in situ* dual reinforcement TiB_2-Ti_2AlC/TiAl composites could be successfully fabricated by using B_4C as the B and C source.
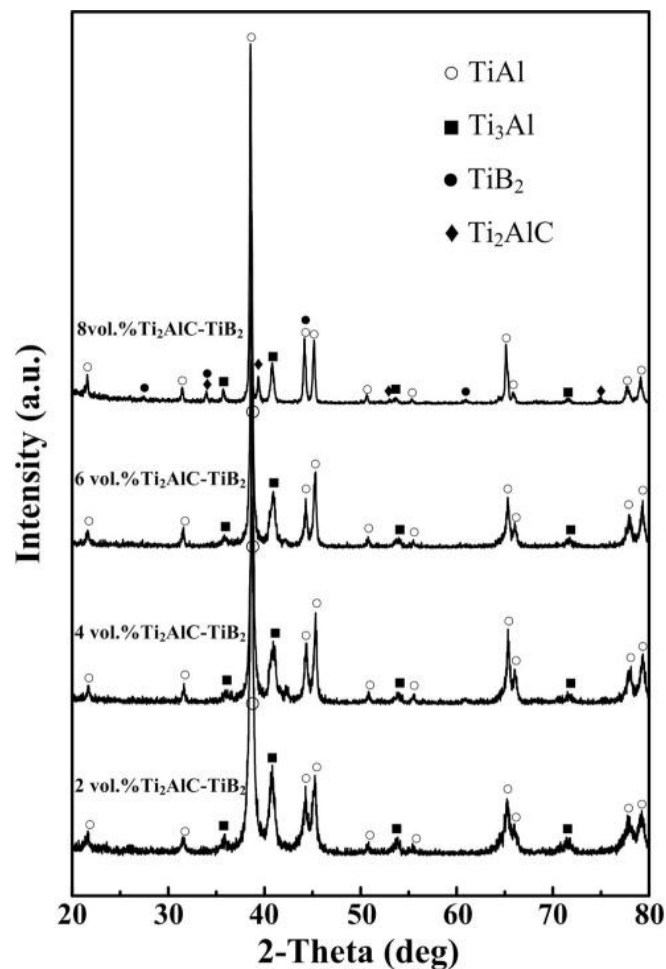
Figure 1. XRD patterns of *in situ* dual reinforcement TiB_2-Ti_2AlC/TiAl composites fabricated by using the Ti-Al-B_4C system.

Figure 2a–d shows the microstructures of the TiB_2-Ti_2AlC/TiAl composites fabricated from the Ti-Al-B_4C system. It can be seen from Figure 2a–c that when the contents of synthesized TiB_2 and Ti_2AlC particles increase from 2–6 vol. %, the ceramic particles distribute more homogeneously in the TiAl matrix. The increasing content of synthesized TiB_2 and Ti_2AlC particles results in more heat released by the reaction and, thus, a higher temperature. The increased temperature facilitates faster and more complete diffusion of the reactants during combustion synthesis, leading to a more uniform distribution of the ceramic particles in the TiAl matrix [17]. However, the ceramic particles begin to sinter together, as shown in Figure 2d, when too many ceramic particles formed in the composites (8 vol. % TiB_2–Ti_2AlC). In order to examine the distribution of TiB_2 and Ti_2AlC particles, EDS was used to distinguish the two ceramic particles from each other (as shown in Figure 2c). It can be seen that in 6 vol. % TiB_2-Ti_2AlC/TiAl composite, Ti_2AlC particles are rod-like in shape with sizes of 1–6 μm in length, while TiB_2 particles are in a near spherical shape with a size of less than 1 μm in diameter.
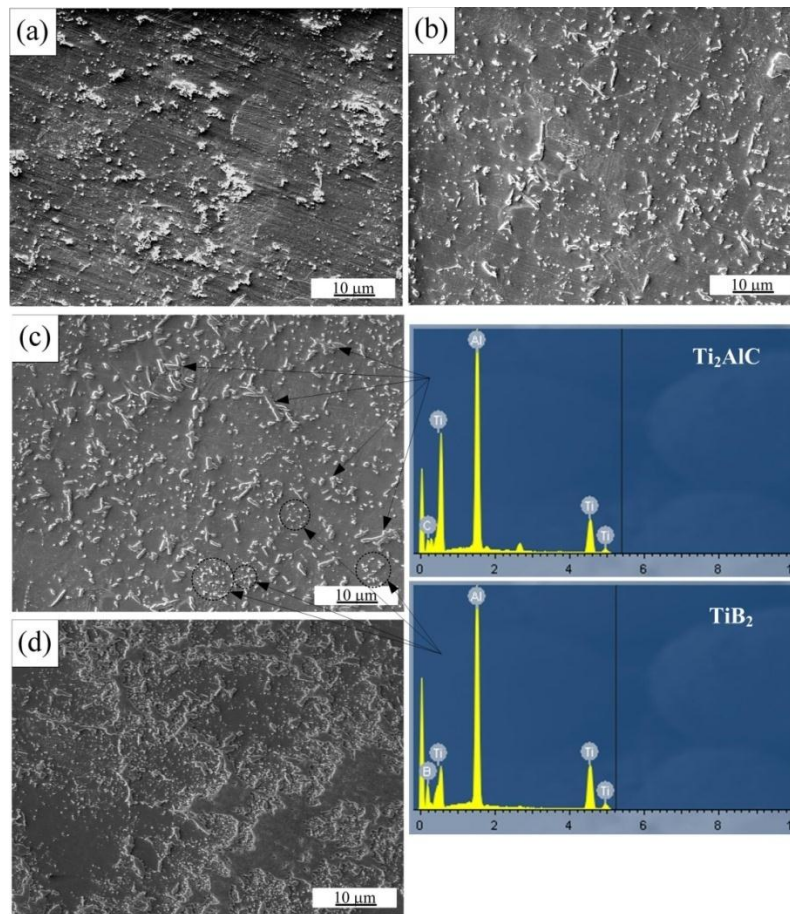
Figure 2. Microstructures of (**a**) 2 vol. % TiB$_2$-Ti$_2$AlC/TiAl; (**b**) 4 vol. % TiB$_2$-Ti$_2$AlC/TiAl; (**c**) 6 vol. % TiB$_2$-Ti$_2$AlC/TiAl and (**d**) 8 vol. % TiB$_2$-Ti$_2$AlC/TiAl composites fabricated by using the Ti-Al-B$_4$C system.

3.2. Compression Properties and Work-Hardening Capacity

Figure 3 shows true compression stress-strain curves of the TiAl alloy and the TiB$_2$-Ti$_2$AlC/TiAl composites fabricated from the Ti-Al-B$_4$C system. The compression properties are summarized in Table 1. The yielding strength (σ_y) and ultimate compression strength (σ_{ucs}) of TiB$_2$-Ti$_2$AlC/TiAl composites increase with increasing content of synthesized ceramic particles. The fracture strain (ε_f) of the composites does not change significantly when the content of synthesized TiB$_2$-Ti$_2$AlC particles increases from 2–6 vol. %. However, when the content of synthesized TiB$_2$-Ti$_2$AlC particles increases to 8 vol. %, ε_f decreases significantly, due to too many ceramic particles being synthesized and segregated together in the composite. This also can be confirmed by the fracture surface of 6 vol. % TiB$_2$-Ti$_2$AlC/TiAl and 8 vol. % TiB$_2$-Ti$_2$AlC/TiAl composites shown in Figure 4a,b. It can be compared to the fracture surface that the 6 vol. % TiB$_2$-Ti$_2$AlC/TiAl composite exhibits with a tear ridge, while the fracture surface of the 8 vol. % TiB$_2$-Ti$_2$AlC/TiAl composite is relatively flat. In 8 vol. % the TiB$_2$-Ti$_2$AlC/TiAl composite, the bad interface combination between aggregated particles and TiAl matrix would play the role of crack initiator during deformation and facilitate the fracture of the composite.
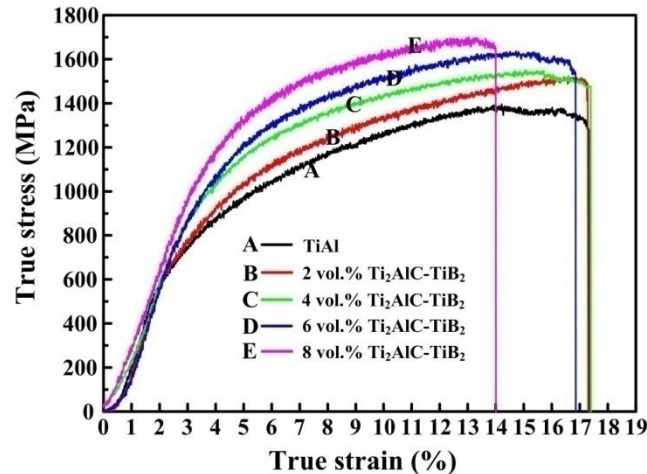
Figure 3. True compression stress-strain curves of TiAl alloy and the *in situ* dual reinforcement TiB$_2$-Ti$_2$AlC/TiAl composites fabricated by using the Ti-Al-B$_4$C system.

Table 1. Compression properties and work-hardening capacity (H_c) of TiAl alloy and the *in situ* dual reinforcement TiB$_2$-Ti$_2$AlC/TiAl composites fabricated by using the Ti-Al-B$_4$C system.

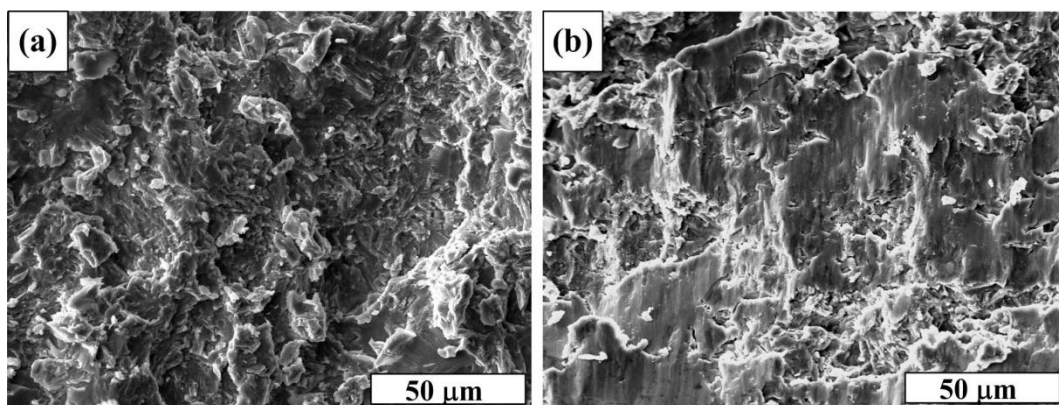| Ceramic Content	Measureddensity (g/cm^3)	σ_y (MPa)	σ_{ucs} (MPa)	ε_f (%)	H_c
TiAl	3.72 $\pm$0.03	465 $\pm$41	1415 $\pm$20	17.3 $\pm$0.0	2.07 $\pm$0.31
2 vol. %	3.74 $\pm$0.02	625 $\pm$24	1487 $\pm$32	16.8 $\pm$0.3	1.39 $\pm$0.15
4 vol. %	3.80 $\pm$0.02	711 $\pm$25	1562 $\pm$10	17.7 $\pm$0.3	1.20 $\pm$0.07
6 vol. %	3.82 $\pm$0.02	781 $\pm$25	1649 $\pm$12	16.6 $\pm$0.2	1.11 $\pm$0.05
8 vol. %	3.88 $\pm$0.05	865 $\pm$29	1695 $\pm$5	14.9 $\pm$0.9	0.96 $\pm$0.06

Figure 4. SEM images of the compression fractured surfaces of (**a**) 6 vol. % and (**b**) 8 vol. % TiB$_2$-Ti$_2$AlC/TiAl composites fabricated by using the Ti-Al-B$_4$C system.

The above results indicate that lower content (2–6 vol. %) TiB$_2$-Ti$_2$AlC particles could effectively improve the strength of TiAl alloy without sacrificing plasticity. The 6 vol. % TiB$_2$-Ti$_2$AlC/TiAl composite possesses the best compression properties. The average σ_y and σ_{ucs} of the 6 vol. % TiB$_2$-Ti$_2$AlC/TiAl composite fabricated by using the Ti-Al-B$_4$C system are 781 MPa and 1649 MPa, respectively, which are 316 MPa and 234 MPa higher than those of TiAl alloy. The enhancement of strength is mainly due to the reinforcing effect of stiff TiB$_2$ and Ti$_2$AlC particles. The uniform

distribution of *in situ* TiB_2 and Ti_2AlC particles would be the reason for the maintenance of the high plasticity. Moreover, as discussed in our previous study [14], the metallic property of Ti_2AlC particles and the coherent interface between Ti_2AlC and TiAl would also contribute to the high plasticity.

It can be seen from the true stress-strain curves of the composites fabricated by using the Ti-Al-B_4C system shown in Figure 3 that these curves all show a clear work hardening. The work-hardening capacity of composites is calculated according to the formulary (H_c) ($H_c = (\sigma_{ucs} - \sigma_y)/\sigma_y$) [18]. The results are listed in Table 1. The H_c of TiB_2-Ti_2AlC/TiAl composite decreases with the increase in the content of synthesized ceramic particles. The onset of plastic deformation with an obvious strain hardening in composites represents a deformation mechanism of dislocation activity. The strain hardening of composites after yielding is mainly due to dislocation multiplication, accumulation and interaction [18–20]. As mentioned above, the σ_y of composites increases with increasing content of synthesized ceramic particles, which means that dislocation-nucleation threshold stress increases with the increase in ceramic content, that is the activation of dislocations becomes more difficult. Consequently, the dislocation interactions during plastic deformation would become weak with the increase in ceramic content, leading to a decrease in H_c. The stress-strain curves also exhibit a low modulus in the elastic region, which is similar to other researchers' work [21,22]. It is speculated that porosity might be playing a part in this. The porosities in the composites evaluated by the method of image analysis are approximately 1.9%, 1.5%, 1.8% and 1.4%, respectively. In addition, the 6 vol. % TiB_2-Ti_2AlC/TiAl composite was also fabricated from the Ti-Al-B-C system, which was used to compare to the composites fabricated from the Ti-Al-B_4C system. Figure 5 shows the true compression stress-strain curves of the *in situ* dual reinforcement 6 vol. % TiB_2-Ti_2AlC/TiAl composites fabricated by these two systems. The compression properties and their work-hardening capacity are summarized in Table 2. The results indicate that the compression properties and work-hardening capacity of the TiB_2-Ti_2AlC/TiAl composites fabricated from these two systems are similar. Thus, from the economic point of view, the TiB_2-Ti_2AlC/TiAl composite fabricated by using the Ti-Al-B_4C system could be widely used in practical production.
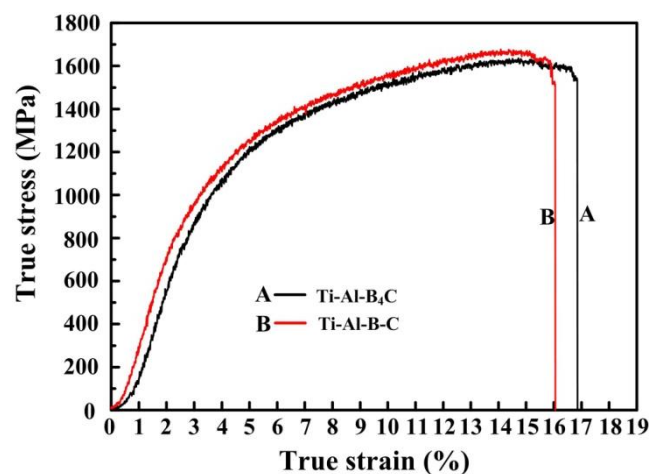

Figure 5. True compression stress-strain curves of the *in situ* dual reinforcement 6 vol. % TiB_2-Ti_2AlC/TiAl composites fabricated by using different systems.

Table 2. Compression properties and work-hardening capacity (H_c) of the *in situ* dual reinforcement TiB$_2$-Ti$_2$AlC/TiAl composites fabricated by using different systems.

System	Ceramic Content	σ_y (MPa)	σ_{ucs} (MPa)	ε_f (%)	H_c
Ti-Al-B$_4$C	6 vol. %	781 $\pm$25	1649 $\pm$12	16.6 $\pm$0.2	1.11 $\pm$0.05
Ti-Al-B-C	6 vol. %	771 $\pm$23	1677 $\pm$1	15.8 $\pm$0.3	1.18 $\pm$0.06

4. Conclusions

The content of TiB$_2$-Ti$_2$AlC particles significantly influences the compression properties and work-hardening capacity of TiAl matrix composites. With the increase in the content of synthesized TiB$_2$-Ti$_2$AlC particles, the σ_y and σ_{ucs} of TiB$_2$-Ti$_2$AlC/TiAl composites increase, while H_c decreases. When the content of synthesized ceramic particles is lower (2 vol. %–6 vol. %), ε_f does not change significantly. However, when the content of ceramic particles comes to 8 vol. %, ε_f decreases significantly. The synthesized TiB$_2$ and Ti$_2$AlC particles could effectively improve the σ_y and σ_{ucs} of TiAl alloy due to the reinforcing effect of stiff TiB$_2$ and Ti$_2$AlC particles. The uniform distribution of *in situ* TiB$_2$ and Ti$_2$AlC particles and the special characteristics of Ti$_2$AlC would be the reasons for the maintenance of the high plasticity. The compression properties of the TiB$_2$-Ti$_2$AlC/TiAl composites fabricated by using the Ti-Al-B$_4$C system are similar to those of the TiB$_2$-Ti$_2$AlC/TiAl composites fabricated by using the Ti-Al-B-C system. From the economic point of view, it is better to fabricate *in situ* dual reinforcement TiB$_2$-Ti$_2$AlC/TiAl composites by using the Ti-Al-B$_4$C system. The σ_y and σ_{ucs} of the 6 vol. % TiB$_2$-Ti$_2$AlC/TiAl composite fabricated by using the Ti-Al-B$_4$C system are 316 MPa and 234 MPa higher than those of the TiAl alloy, without sacrificing plasticity.

Author Contributions

These authors accomplished this work together.

Conflicts of Interest

The authors declare no conflict of interest.

References

1. Kumar, K.S.; Bao, G. Intermetallic-matrix composites: An overview. *Compos. Sci. Technol*. **1994**, *52*, 127–150.

2. Xiang, L.Y.; Wang, F.; Zhu, J.F.; Wang, X.F. Mechanical properties and microstructure of Al_2O_3/TiAl *in situ* composites doped with Cr_2O_3. *Mater. Sci. Eng. A* **2011**, *528*, 3337–3341.

3. Rao, K.P.; Zhou, J.B. Characterization and mechanical properties of *in situ* synthesized Ti_5Si_3/TiAl composites. *Mater. Sci. Eng. A* **2003**, *356*, 208–218.

4. Yang, C.H.; Wang, F.; Ai, T.T.; Zhu, J.F. Microstructure and mechanical properties of *in situ* TiAl/Ti_2AlC composites prepared by reactive hot pressing. *Ceram. Int*. **2014**, *40*, 8165–8171.

5. Ai, T.T.; Wang, F.; Feng, X.M.; Ruan, M.M. Microstructural and mechanical properties of dual Ti_3AlC_2-Ti_2AlC reinforced TiAl composites fabricated by reaction hot pressing. *Ceram. Int*. **2014**, *40*, 9947–9953.

6. Li, B.; Lavernia, E.J. Spray forming and co-injection of particulate reinforced TiAl/TiB_2 composites. *Acta Mater*. **1997**, *45*, 5015–5030.

7. Van Meter, M.L.; Kampe, S.L.; Christodoulou, L. Mechanical properties of near-γ titanium aluminides reinforced with high volume percentages of TiB_2. *Scr. Mater*. **1996**, *34*, 1251–1256.

8. Hirose, A.; Hasegawa, M.; Kobayashi, K.F. Microstructures and mechanical properties of TiB_2 particle reinforced TiAl composites by plasma arc melting process. *Mater. Sci. Eng. A* **1997**, *239–240*, 46–54.

9. Bohn, R.; Klassen, T.; Bormann, R. Room temperature mechanical behavior of silicon-doped TiAl alloys with grain sizes in the nano-and submicron-range. *Acta Mater*. **2001**, *49*, 299–311.

10. Kim, S.H.; Chung, H.H.; Pyo, S.G.; Hwang, S.J.; Kim, N.J. Effect of B on the Microstructure and Mechanical Properties of Mechanically Milled TiAl Alloys. *Metall. Mater. Trans. A* **1998**, *29*, 2273–2283.

11. Lin, Z.J.; Zhuo, M.J.; Zhou, Y.C.; Li, M.S.; Wang, Y.J. Microstructural characterization of layered ternary Ti_2AlC. *Acta Mater.* **2006**, *54*, 1009–1015.

12. Chen, Y.L.; Yan, M.; Sun, Y.M.; Mei, B.C.; Zhu, J.Q. The phase transformation and microstructure of TiAl/Ti_2Al composites caused by hot pressing. *Ceram. Int.* **2009**, *35*, 1807–1812.

13. Kulkarni, S.R.; Datye, A.V.; Wu, K.-H. Synthesis of Ti_2AlC by spark plasma sintering of TiAl-carbon nanotube powder mixture. *J. Alloys Compd*. **2010**, *490*, 155–159.

14. Shu, S.L.; Qiu, F.; Lü, S.J.; Jin, S.B.; Jiang, Q.C. Phase transitions and compression properties of Ti_2AlC/TiAl composites fabricated by combustion synthesis reaction. *Mater. Sci. Eng. A* **2012**, *539*, 344–348.

15. Yang, F.; Kong, F.T.; Chen, Y.Y.; Xiao, S.L. Effect of spark plasma sintering temperature on the microstructure and mechanical properties of a Ti_2AlC/TiAl composite. *J. Alloys Compd*. **2010**, *496*, 462–466.

16. Shu, S.L.; Qiu, F.; Lin, Y.; Wang, Y.; Wang, J.; Jiang, Q. Effect of B_4C size on the fabrication and compression properties of *in situ* TiB_2-Ti_2AlC/TiAl composites. *J. Alloys Compd*. **2013**, *551*, 88–91.

17. Alman, D.E. Reactive sintering of TiAl-Ti$_5$Si$_3$ *in situ* composites. *Intermetallics* **2005**, *13*, 572–579.

18. Afrin, N.; Chen, D.L.; Cao, X.; Jahazi, M. Strain hardening behavior of a friction stir welded magnesium alloy. *Scr. Mater.* **2007**, *57*, 1004–1007.

19. Sun, B.B.; Sui, M.L.; Wang, Y.M.; He, G.; Eckert, J.; Ma, E. Ultrafine composite microstructure in a bulk Ti alloy for high strength, strain hardening and tensile ductility. *Acta Mater.* **2006**, *54*, 1349–1357.

20. Zhao, Y.H.; Bingert, J.F.; Liao, X.Z.; Cui, B.Z.; Han, K.; Sergueeva, A.V.; Mukherjee, A.K.; Valiev, R.Z.; Langdon, T.G.; Zhu, Y.T. Simultaneously increasing the ductility and strength of nano structured alloys. *Adv. Mater.* **2006**, *18*, 2949–2953.

21. Calderon, H.A.; Garibay-Febles, V.; Umemoto, M.; Yamaguchi, M. Mechanical properties of nanocrystalline Ti-Al-X alloys. *Mater. Sci. Eng. A* **2002**, *329–331*, 196–205.

22. Rao, K.P.; Vyas, A. Comparison of titanium silicide and carbide reinforced *in situ* synthesized TiAl composites and their mechanical properties. *Intermetallics* **2011**, *19*, 1236–1242.